

Magnetic structures in $\text{Pr}_6\text{Ni}_2\text{Si}_3$ and $\text{Pr}_5\text{Ni}_2\text{Si}_3$

D. C. Jiles^{a)}*Wolffson Centre for Magnetics, Cardiff University, Cardiff CF24 3AA, United Kingdom*

S. H. Song

Materials Science and Engineering Department, Iowa State University, Ames, Iowa 50011 and Materials and Engineering Physics Program, Ames Laboratory, Ames, Iowa 50011

(Received 27 June 2006; accepted 7 September 2006; published online 30 January 2007)

The temperature dependence of magnetization in $\text{Pr}_6\text{Ni}_2\text{Si}_3$ and $\text{Pr}_5\text{Ni}_2\text{Si}_3$ compounds has been studied with the objective of providing a theoretical understanding of the behavior of the magnetic properties of the material. The ternary Pr–Ni–Si system contains the homologous series of compounds $R_{(n+2)(n+1)}\text{Ni}_{n(n-1)+2}\text{Si}_{n(n+1)}$, where R is a rare earth element which provides a range of materials with different but related structures. The crystal structures and unit cells of $\text{Pr}_6\text{Ni}_2\text{Si}_3$ ($n=2$) and $\text{Pr}_5\text{Ni}_2\text{Si}_3$ ($n=3$) compounds are closely related consisting of an overall hexagonal structure comprising trigonal columns of atoms, in which the only difference is in the size of the triangular base of the column which depends directly on the chemical composition, specifically the index n . The calculations were based on a nearest neighbor exchange interaction approximation under two kinds of conditions: collinear and noncollinear magnetic structures. The results of these calculations show the Curie temperature, but do not yet predict quantitatively the spin reorientation transition at lower temperatures. © 2007 American Institute of Physics. [DOI: 10.1063/1.2388043]

I. INTRODUCTION

A “model system” in materials science needs to satisfy at least three conditions: (1) the system must be simple enough that there are only a few dominant factors which influence the physical property to be studied or predicted, (2) the factors (such as composition, crystal structure, temperature, pressure, or exchange interaction) that are ultimately responsible for the physical phenomena can be controlled in a well defined way so that their effects can be studied independently, and (3) the predictions obtained from the model system should be testable. To be useful the results should be applicable to other related cases. In this respect the Pr–Ni–Si alloy system can serve as a model system for the study of structure/property relationships in magnetic materials.

The ternary Pr–Ni–Si alloy system is one member of a more general system of alloys and compounds which form a homologous series of the type $R_{(n+2)(n+1)}\text{Ni}_{n(n-1)+2}\text{Si}_{n(n+1)}$, where R is a rare earth element. Pr–Ni–Si provides a range of materials with different structures as described by Rogl.¹ Overall the alloy system exhibits a hexagonal crystal structure formed of subassemblies of trigonal prismatic columns. The number of smaller triangular arrays that fits along each side to form the basal plane of the larger trigonal prism of the unit cell is determined by the value of n in the chemical formula. Identifiable compounds “ $\text{Pr}_6\text{Ni}_2\text{Si}_3$ ” ($n=2$), “ $\text{Pr}_5\text{Ni}_2\text{Si}_3$ ” ($n=3$), and “ $\text{Pr}_{15}\text{Ni}_7\text{Si}_{10}$ ” ($n=4$) have been prepared and are members of this series.

The trigonal prisms containing the local arrays of Pr atoms can be considered as “magnetic clusters.” The size of these clusters can be controlled by selection of the chemical composition. As the chemical composition changes (and

hence the size of the magnetic clusters changes), the number of nearest neighbors (and hence the exchange interactions) for each Pr atom site also changes systematically. Therefore the physical properties vary systematically from one member of the series to the next.

Experimental results on the magnetic properties of $\text{Pr}_5\text{Ni}_2\text{Si}_3$ and $\text{Pr}_{15}\text{Ni}_7\text{Si}_{10}$ polycrystalline samples and a $\text{Pr}_5\text{Ni}_2\text{Si}_3$ single crystal sample have recently been reported.^{2–6} Each compound showed two magnetic phase transitions: a magnetic order/disorder transition at a higher temperature (41 K for $\text{Pr}_5\text{Ni}_2\text{Si}_3$, and 58 K for $\text{Pr}_{15}\text{Ni}_7\text{Si}_{10}$) and another transition, which exhibits the characteristics of spin reorientation transition, at a lower temperature (25 K for $\text{Pr}_5\text{Ni}_2\text{Si}_3$ and 31 K for $\text{Pr}_{15}\text{Ni}_7\text{Si}_{10}$).

The present paper reports on the theoretical investigation to attempt to explain the temperature dependent magnetization of $\text{Pr}_6\text{Ni}_2\text{Si}_3$ ($n=2$) and $\text{Pr}_5\text{Ni}_2\text{Si}_3$ ($n=3$) compounds. The calculations are based on a nearest neighbor exchange interaction approximation under two kinds of conditions: collinear and noncollinear magnetic structures. The crystal structures and unit cells of $\text{Pr}_6\text{Ni}_2\text{Si}_3$ and $\text{Pr}_5\text{Ni}_2\text{Si}_3$ compounds are shown in Figs. 1(a) and 1(b), respectively.

II. THEORETICAL BASIS FOR MODEL CALCULATIONS

In order to calculate the expected variation of magnetization with temperature (M vs T) in Pr–Ni–Si single crystal, the exchange interaction energy for each atomic site was determined using a nearest neighbor exchange interaction approximation. For this calculation, the following were assumed:

- (1) Only the Pr atoms have a magnetic moment and therefore only these atoms contribute to magnetization.
- (2) The magnetic moment per Pr atom is $3.58\mu_B$.

^{a)}Electronic mail: jilesd@cf.ac.uk

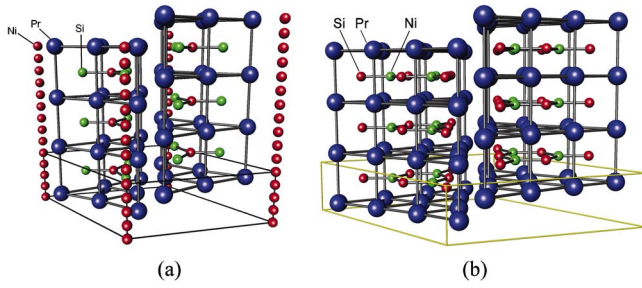


FIG. 1. (Color online) Crystal structure and unit cell of (a) $\text{Pr}_6\text{Ni}_2\text{Si}_3$ ($n=2$) and (b) $\text{Pr}_5\text{Ni}_2\text{Si}_3$ ($n=3$) showing the trigonal cells which form prismatic columnar assemblies. [Note that in the case of $\text{Pr}_5\text{Ni}_2\text{Si}_3$ there are additional Ni atoms not shown here for the purposes of simplicity. These lie at the corner of the rhombohedra containing the two trigonal prisms and amount to one extra Ni atom per trigonal plane as shown in (a).]

- (3) The exchange interaction exists only between the nearest neighbors, which is expressed in terms of the exchange energy according to the following equation:

$$E_{\text{ex}} = -2J_{\text{NN}} \sum_{i,j} J_i J_j, \quad (1)$$

where J_{NN} is the exchange interaction coefficient between nearest neighbors and J_i and J_j are the total angular momentum at the i th and j th sites, respectively.

A. $\text{Pr}_6\text{Ni}_2\text{Si}_3$

For the purposes of calculation the arrangement of Pr atoms in the crystal structure was transformed into an orthogonal coordinate system as shown in Fig. 2(a), from which the distances between various Pr atom pairs were calculated. The results show that the distances vary between the different types of Pr atom pairs. The Pr atoms less than 0.5 nm apart were selected as “nearest neighbors” for the purposes of these calculations. The specific atomic position and the distances of nearest neighbors from each type of Pr atom are shown in Table I. The Pr atoms in the triangular base plane of the columnar structure of $\text{Pr}_6\text{Ni}_2\text{Si}_3$ compound

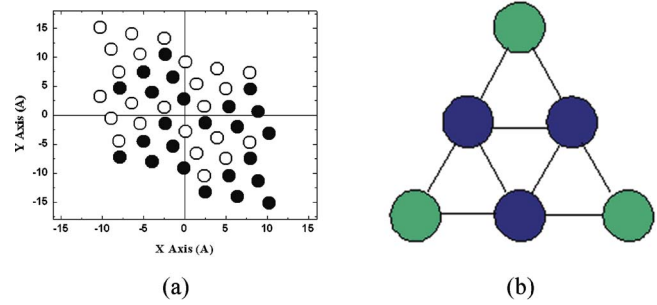


FIG. 2. (Color online) (a) The projection of Pr atoms on the base plane in the crystal structure of $\text{Pr}_6\text{Ni}_2\text{Si}_3$ compound. The solid and open circles indicate the Pr atoms in successive planes, above and below, the distance between which is half of the unit cell’s height along the c axis, respectively. (b) Diagram of the trigonal base plane in $\text{Pr}_6\text{Ni}_2\text{Si}_3$ showing two types of Pr atoms—green and blue circles indicate “corner” and “edge” atoms, respectively.

can be classified into two groups depending on the number of nearest neighbors that they have among Pr atoms. It can be shown that Pr atoms along the edges of the triangular plane have ten nearest neighbors and those at the corners of the triangular plane have 12 nearest neighbors. The arrangement of Pr atoms in the base plane of the $\text{Pr}_6\text{Ni}_2\text{Si}_3$ compound is shown in Fig. 2(b). The three-dimensional arrangement of nearest neighbor Pr atoms is shown in Fig. 3 for (a) “edge” and (b) “corner” atoms.

The average exchange interaction energy between nearest neighbors was calculated based on the experimentally measured Curie temperature ($T_C=40$ K),⁷

$$E_{\text{ex}}^{\text{triangle}} = 3J_{\text{NN}} \sum_{i,j}^{\text{edge atom}} J_i J_j + 3J_{\text{NN}} \sum_{i,j}^{\text{corner atom}} J_i J_j, \quad (2)$$

where $E_{\text{ex}}^{\text{triangle}}$ is the total exchange energy for each triangular base plane in the unit cell, such as the one shown in Fig. 2(b). This energy corresponds to $18k_B T_C$, the thermal energy that six Pr atoms in the triangular base plane have at the Curie temperature in order to cause the transition from a ferromagnetic to a paramagnetic state ($6 \text{ Pr atoms} \times 3k_B T_C$).

TABLE I. The atomic positions and the distances of nearest neighbors from each type of Pr atom in $\text{Pr}_6\text{Ni}_2\text{Si}_3$.

Type of Pr atom	Atomic position of nearest neighbor	Distance (Å)	Type of Pr atom	Atomic position of nearest neighbor	Distance (Å)
Corner atom (with 12 nearest neighbor Pr atoms)	Two corner atoms on neighboring columns 1/2 plane up	3.53	Edge atom (with ten nearest neighbor Pr atoms)	One corner atom on neighboring column 1/2 plane up	3.70
	Two corner atoms on neighboring columns 1/2 plane down	3.53		One corner atom on neighboring column 1/2 plane down	3.70
	One edge atom on neighboring columns 1/2 plane up	3.70		One edge atom on neighboring column 1/2 plane up	3.78
	One edge atom on neighboring columns 1/2 plane down	3.70		One edge atom on neighboring column 1/2 plane down	3.78
	Two edge atoms in the same column and plane	4.0		Two corner atoms in the same column and plane	4.0
	Two corner atoms on neighboring columns in the same plane	4.85		Two edge atoms in the same column and plane	3.64
	One corner atom in the same column, the next plane up	4.28		One edge atom in the same column, the next plane up	4.28
	One corner atom in the same column, the next plane down	4.28		One edge atom in the same column, the next plane down	4.28

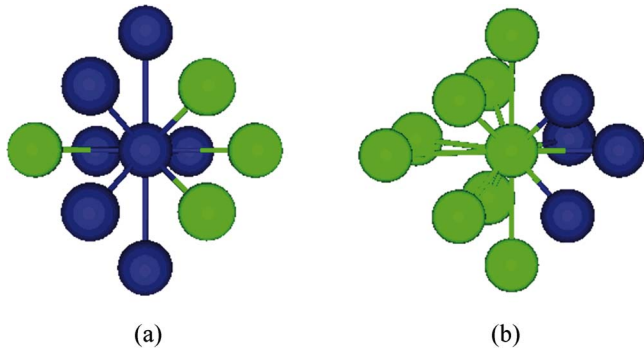


FIG. 3. (Color online) Arrangement of nearest neighbor Pr atoms around (a) edge and (b) corner atoms in $\text{Pr}_6\text{Ni}_2\text{Si}_3$. Green and blue circles indicate corner and edge Pr atoms, respectively.

Since the effective magnetic field that each atom experiences depends on the number of nearest neighbors for each site, the effective magnetic field for each atomic site can be expressed as

$$E_{\text{ex}}^{\text{site}} = -J_{\text{NN}} \sum_{i,j}^{\text{site}} J_{ij} = m\mu_0 H_{\text{eff}}^{\text{site}} = m\mu_0 \alpha_{\text{site}} M, \quad (3)$$

where $H_{\text{eff}}^{\text{site}}$ is the exchange field for each site and α_{site} is the mean field coefficient for each site. Assuming that the exchange field can be rewritten in the form $H_{\text{eff}}^{\text{site}} = \alpha_{\text{site}} M$, the total magnetic moment per triangular base plane can be expressed as the vector sum of all the edge (e) and corner or apex (a) moments in the base plane,

$$m^{\text{triangle}} = m^e + m^a = 3m_0 B_J \left[\frac{m_0 \mu_0 (H + H_{\text{eff}}^e)}{k_B T} \right] + 3m_0 B_J \left[\frac{m_0 \mu_0 (H + H_{\text{eff}}^a)}{k_B T} \right], \quad (4)$$

where m^e is the sum of magnetic moments of the three Pr atoms located on the edges in the trigonal base plane, m^a is the sum of magnetic moments of the three Pr atoms located on the corners in the trigonal base plane, and $B_J(x)$ is the Brillouin function,

$$B_J(x) = \left(\frac{2J+1}{2J} \right) \coth \left[\frac{(2J+1)x}{2J} \right] - \left(\frac{1}{2J} \right) \coth \left(\frac{x}{2J} \right). \quad (5)$$

B. $\text{Pr}_5\text{Ni}_2\text{Si}_3$

Calculations for the $\text{Pr}_5\text{Ni}_2\text{Si}_3$ compound have been performed in two different ways based on two different assumptions: (a) collinear alignment and (b) noncollinear alignment of magnetic moments. The calculation procedure for collinear magnetic moments is analogous to that for the $\text{Pr}_6\text{Ni}_2\text{Si}_3$ compound, although the structure of $\text{Pr}_5\text{Ni}_2\text{Si}_3$ is more complicated than $\text{Pr}_6\text{Ni}_2\text{Si}_3$. The Pr atoms in the triangular base plane of the columnar structure of $\text{Pr}_5\text{Ni}_2\text{Si}_3$ ($n=3$) compound were classified into three groups, corner (or apex) a , edge e , and center c depending on the number of nearest neighbor Pr atoms.

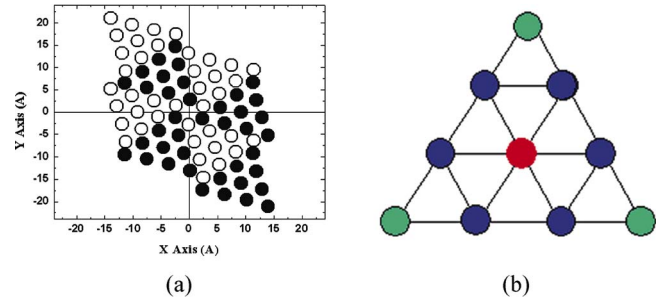


FIG. 4. (Color online) (a) The projection of Pr atoms on the base plane in the crystal structure of $\text{Pr}_5\text{Ni}_2\text{Si}_3$ ($n=3$) compound. The solid and open circles indicate the Pr atoms in the successive array of planes, above and below, the distance between which is half of the unit cell's height along the c axis. (b) Diagram of the trigonal base plane in $\text{Pr}_5\text{Ni}_2\text{Si}_3$ showing three types of Pr atoms—green, blue, and red circles indicate the corner, edge, and center atoms, respectively.

For the purposes of calculation the arrangement of Pr atoms in the crystal structure was transformed into an orthogonal coordinate system as shown in Fig. 4(a), from which the distances between various Pr atom pairs were calculated. Pr atoms at the center sites of the triangular plane have eight nearest neighbors, those along the edges of the triangular plane have ten nearest neighbors, and those at the corners of the triangular plane have 12 nearest neighbors. This is shown in Figs. 4(a) and 4(b). Figure 5 and Table II show the atomic arrangement and distances of each type of Pr atom from the nearest neighbors, respectively.

1. Collinear alignment

The exchange interaction energy is calculated from the equation

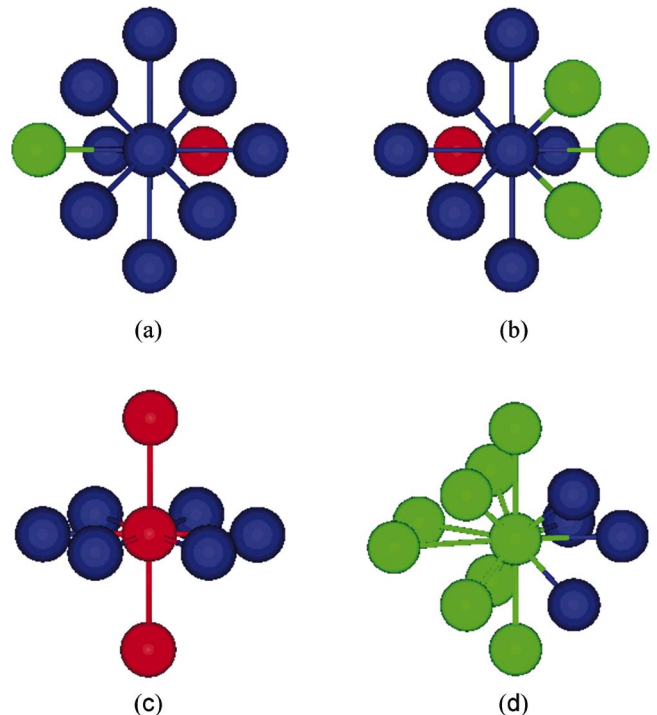


FIG. 5. (Color online) Arrangement of nearest neighbor Pr atoms around the (a) edge (A), (b) edge (B), (c) center, and (d) corner Pr atoms in $\text{Pr}_5\text{Ni}_2\text{Si}_3$ ($n=3$) compound. Green, blue, and red circles indicate corner, edge, and center, Pr atoms, respectively.

TABLE II. The atomic positions and the distances of nearest neighbors from each type of Pr atom in Pr₅Ni₂Si₃.

Type of Pr atom	Atomic position of nearest neighbor	Distance (Å)	Type of Pr atom	Atomic position of nearest neighbor	Distance (Å)				
Corner atom (with 12 nearest neighbor Pr atoms)	Two corner atoms on neighboring columns 1/2 plane up	3.51	Center atom (with 8 nearest neighbor Pr atoms)	Six edge atoms in the same column and plane	3.82–3.88				
	Two corner atoms on neighboring columns 1/2 plane down	3.51		One center atom in the same column, the next plane up					
	One edge atom on neighboring column 1/2 plane up	3.70							
	One edge atom on neighboring column 1/2 plane down	3.70							
	Two edge atoms in the same column and plane	4.05			One center atom in the same column, the next plane down				
	Two corner atoms on neighboring columns, in the same plane	4.84							
	One corner atom in the same column, the next plane up	4.25				Edge (B) atom (with ten nearest neighbor Pr atoms)	One corner atom on neighboring column 1/2 plane up	3.70	
	One corner atom in the same column, the next plane down	4.25					One corner atom on neighboring column 1/2 plane down	3.70	
	Edge (A) atom (with ten nearest neighbor Pr atoms)	Two edge atoms on neighboring columns 1/2 plane up					3.80	One edge atom on neighboring column 1/2 plane up	3.80
		Two edge atoms on neighboring columns 1/2 plane down					3.80	One edge atom on neighboring column 1/2 plane down	3.80
One corner atom in the same column and plane		4.05	Two edge atoms in the same column and plane				3.63/4.07		
Two edge atoms in the same column and plane		3.63/4.05		One center atom in the same column and plane			3.82		
One center atom in the same column and plane		3.88		One corner atom in the same column and plane			4.05		
One edge atom in the same column, the next plane up		4.25		One edge atom in the same column, the next plane up			4.25		
One edge atom in the same column, the next plane down		4.25		One edge atom in the same column, the next plane down	4.25				

$$E_{\text{ex}} = -2J_{\text{NN}} \sum_{i,j} J_i J_j \cos \theta_{i,j}, \quad (6)$$

where θ is the angle between magnetic moments at i th and j th sites. The total exchange interaction energy per unit triangular plane can be obtained using the measured Curie temperature (T_C),

$$E_{\text{ex}}^{\text{triangle}} = 1J_{\text{NN}} \sum_{i,j}^{\text{center atom}} J_i J_j + 6J_{\text{NN}} \sum_{i,j}^{\text{edge atom}} J_i J_j + 3J_{\text{NN}} \sum_{i,j}^{\text{corner atom}} J_i J_j = 30k_B T_C. \quad (7)$$

Based on this equation the magnetization versus temperature curve (M vs T) was calculated following the same method as in the Pr₆Ni₂Si₃ case. It should be noted that the exchange energy for each atom depends on its location in the triangular plane because of the different numbers of nearest neighbors. This means that different Pr atoms in the triangular base plane will have their magnetic moments held in their orientations with different energies depending on their location in the plane.

2. Noncollinear alignment

The calculation for noncollinear magnetic moments is significantly more complicated than for collinear moments.

In order to perform this calculation the Pr atoms in the lattice need to be classified into four separate groups, although the number of nearest neighbor Pr atoms per site remains the same as for the collinear case. According to neutron diffraction data,⁸ the component of the magnetic moment of the corner Pr atom along the c axis is $0.72\mu_B$, which can be interpreted to mean that the magnetic moments of the corner atoms are tilted 78° away from the c axis. From this the angles between the magnetic moments for each Pr site were calculated and these were then included in the subsequent calculation of the exchange interaction energy using Eq. (6) above.

Considering these noncollinear effects on the exchange interaction energy, the edge atoms can be further classified into two subgroups based on the fact that the angle between magnetic moments of “edge-corner” atom pairs is different than that of “edge-edge” atom pairs, and that “edge (A)” and “edge (B)” atoms have different combinations of nearest neighbor Pr atoms. For edge (A) type there are eight edge/one center/one corner nearest neighbor atoms while for edge (B) type there are six edge/one center/three corner nearest neighbor atoms. Therefore for the noncollinear calculation the contribution to total exchange energy for each atom is not a simple linear function of the number of nearest neighbors for each site, but a more complicated function of two variables, N (the number of nearest neighbors) and θ (the relative angle of orientation between neighboring pairs). Figure 5 and

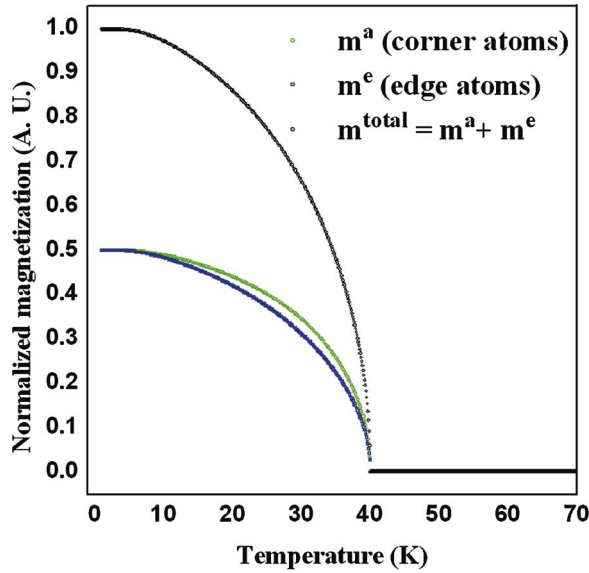


FIG. 6. (Color online) Calculated M vs T curves using Brillouin functions for the $\text{Pr}_6\text{Ni}_2\text{Si}_3$ compound. Green and blue symbols represent the magnetization due to the Pr atoms at corner and edge sites, respectively. The black symbols are the sum of these two contributions, which correspond to the total magnetization.

Table II were used to determine how many nearest neighbor atoms should be used in the calculation. The total exchange interaction energy per triangular base plane was then calculated as follows:

$$\begin{aligned}
 E_{\text{ex}}^{\text{triangle}} &= E_{\text{ex}}^{\text{center}} + E_{\text{ex}}^{\text{edge A}} + E_{\text{ex}}^{\text{edge B}} + E_{\text{ex}}^{\text{corner}} \\
 &= 1J_{\text{NN}} \sum_{i,j}^{\text{center atom}} J_i J_j \cos \theta_{i,j} \\
 &\quad + 3J_{\text{NN}} \sum_{i,j}^{\text{edge A atom}} J_i J_j \cos \theta_{i,j} \\
 &\quad + 3J_{\text{NN}} \sum_{i,j}^{\text{edge B atom}} J_i J_j \cos \theta_{i,j} \\
 &\quad + 3J_{\text{NN}} \sum_{i,j}^{\text{corner atom}} J_i J_j \cos \theta_{i,j} = 30k_B T_C. \quad (8)
 \end{aligned}$$

III. RESULTS AND DISCUSSIONS

A. $\text{Pr}_6\text{Ni}_2\text{Si}_3$

The calculated magnetization versus temperature (M vs T) curves for each type of Pr atom as well as the total resultant magnetic moment for $\text{Pr}_6\text{Ni}_2\text{Si}_3$ are shown in Fig. 6. The magnetization curve for each type of Pr atom in the triangular base plane has been presented in terms of normalized magnetization compared with the total magnetization. The calculated M vs T curve for each type of Pr atom is indicated with green (corner) and blue (edge) symbols and the total magnetization curve with black symbols. All curves show a monotonic decrease of M with T over the entire range of temperature and a Curie temperature of 40 K which is consistent with the experimentally measured value. However, the rate of decrease in magnetization with temperature is

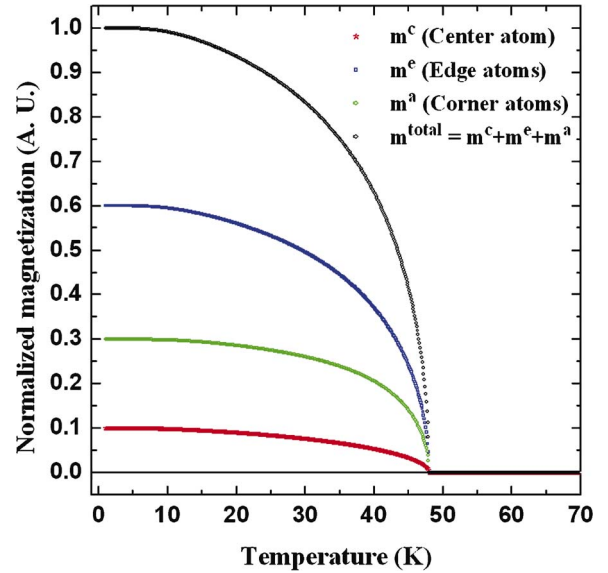


FIG. 7. (Color online) Calculated M vs T curves using Brillouin functions for the $\text{Pr}_5\text{Ni}_2\text{Si}_3$ compound with collinear magnetic moments. Red/blue/green symbols represent the magnetization due to the Pr atoms at the center/edge/corner sites, respectively. The black symbols are the sum of these three contributions, which correspond to the resultant total magnetization of this compound.

different for each type of Pr atoms. Magnetization for edge atoms decreases faster with temperature than for corner atoms. This is due to the difference in number of nearest neighbor exchange interactions for the two different types of Pr atom, ten for edge atoms and 12 for corner atoms, thus making a difference in the exchange field ($H_{\text{eff}}^{\text{site}}$) for the different atomic sites.

B. $\text{Pr}_5\text{Ni}_2\text{Si}_3$

1. Collinear magnetic moments

The calculated magnetization versus temperature (M vs T) curves for each of the different types of Pr atoms as well as the total magnetic moments for $\text{Pr}_5\text{Ni}_2\text{Si}_3$ compound have been calculated using the same method as with the $\text{Pr}_6\text{Ni}_2\text{Si}_3$ case, based on the assumption that all magnetic moments are collinear. The calculated M vs T curves are shown in Fig. 7, in which the red/blue/green symbols represent the contributions of center/edge/corner atoms to the magnetization, and the black symbols represent the resultant total magnetization. The results show a monotonic decrease of M with T over the entire range of temperature. This is similar to that of the $\text{Pr}_6\text{Ni}_2\text{Si}_3$ compound. The calculated Curie temperature of 48 K is consistent with the experimentally measured value. The rate of decrease in magnetization with temperature is different for each of the different types of Pr atom, which is due to the difference in the number of nearest neighbors for each of the different types of Pr site leading to a difference in the exchange field ($H_{\text{eff}}^{\text{site}}$) for the different atomic sites

2. Noncollinear magnetic moments

The experimentally determined magnetization versus temperature (M vs T) curves of $\text{Pr}_5\text{Ni}_2\text{Si}_3$ single crystal are shown in Figs. 8(a) and 8(b), where M was measured (a)

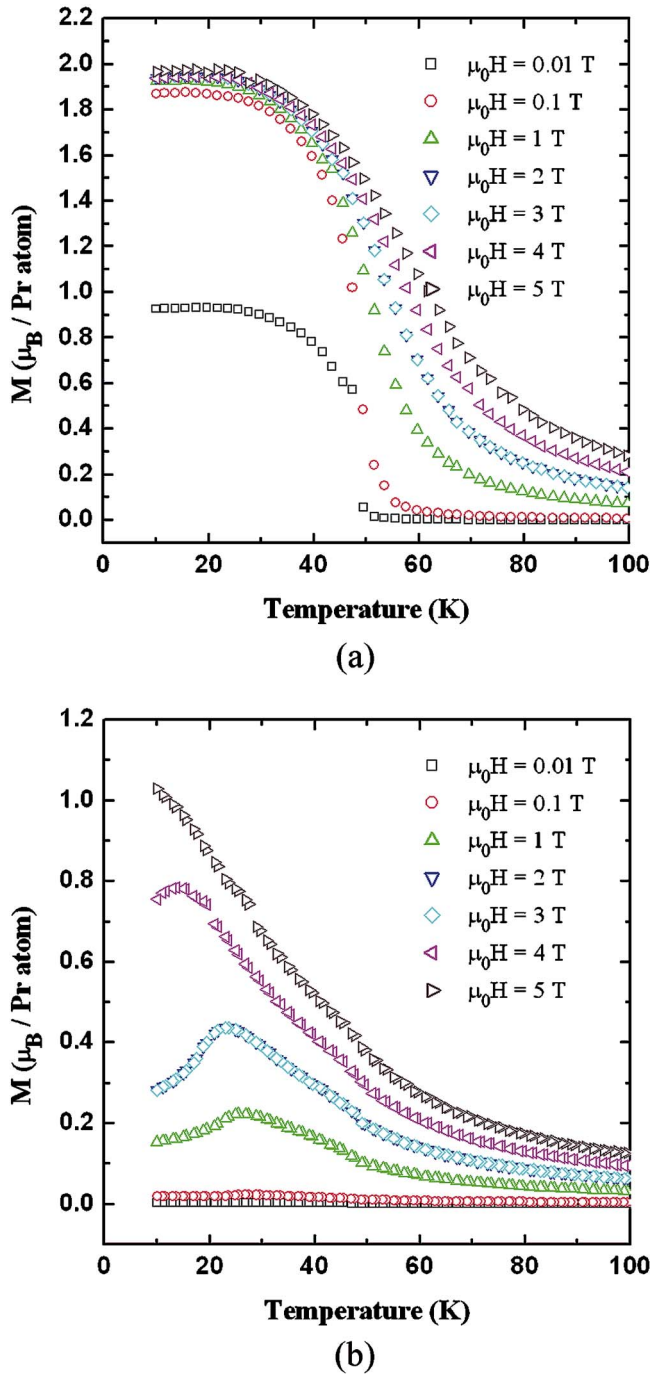


FIG. 8. (Color online) Variation of the magnetization of $\text{Pr}_5\text{Ni}_2\text{Si}_3$ single crystal with temperature, measured (a) parallel $M_{\parallel c}$ and (b) perpendicular $M_{\perp c}$ to the c axis under various strengths of applied magnetic field (Ref. 7).

parallel and (b) perpendicular to the c axis using a superconducting quantum interference device (SQUID) magnetometer.⁷ These magnetizations are shown in terms of the net number of Bohr magnetons per Pr atom. The magnetic moment per Pr atom in the single ion state is $3.58 \mu_B$. In the condensed matter state the value of this moment is likely to be different as indicated by preliminary experimental measurements using neutron diffraction.⁸ In fact it appears that the Pr atoms on each of the three different types of lattice sites have different magnetic moments.

The fact that the maximum value of magnetization under a field of $\mu_0 H = 5$ T was 55% of expected saturation for the

component of magnetization parallel to the c axis $M_{\parallel c}$ and 29% of expected saturation for the component of magnetization perpendicular to the c axis $M_{\perp c}$ indicates that the values of magnetization measured in both directions are not saturated even at a field of $\mu_0 H = 5$ T and that the easy axis may be closer to the c axis than to the base plane. This can be explained by considering the atomic arrangement of Pr atoms. In the case of a Pr atom at the corner site, the Pr atom has 12 nearest neighbors as shown in Fig. 5(d). This also shows that the atomic arrangement of nearest neighbors around the Pr atom at the corner site is not symmetric and further suggests that the magnetic moments at the corner Pr atoms will tend to be tilted away from the c axis.

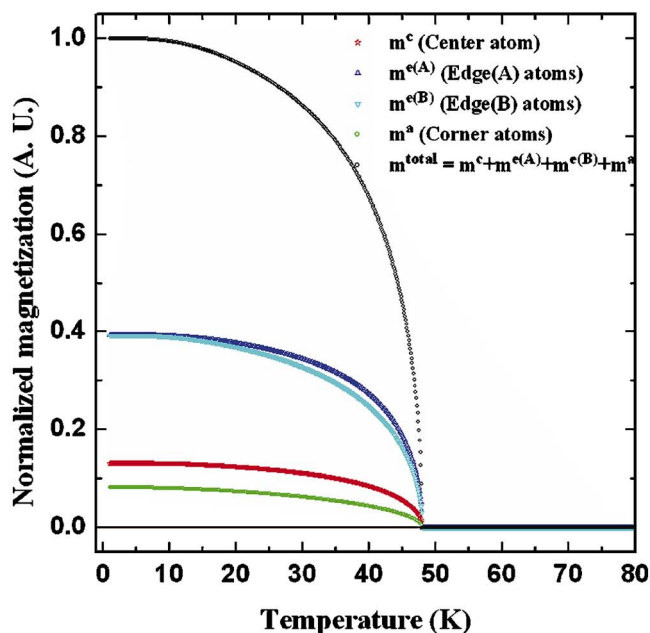
These predictions are also consistent with the neutron diffraction data which indicate that the component of magnetic moment along the c axis of the Pr atom at the corner site is $0.72 \mu_B$. This could be interpreted to mean that the magnetic moment of the corner atoms is tilted 78° away from the c axis. Based on this the possible angles between the magnetic moments for each site were calculated and these were included in the calculation of the exchange interaction energy using Eq. (6).

The expected M vs T curves for each type of Pr atom were calculated. The results are shown in Fig. 9(a), which predicts a consistent Curie temperature for all sites, which agrees with the experimental results shown in Fig. 8. From results of the calculated M vs T curves shown in Fig. 9(a) the expected variation with temperature of the average angle of magnetic moment relative to the c axis for each type of Pr atom has been calculated and is shown in Fig. 9(b).

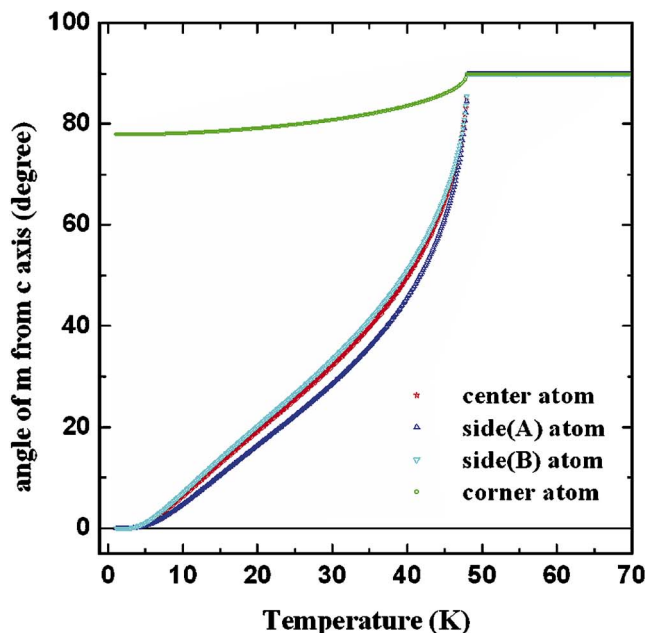
When it comes to the experimentally measured $M_{\perp c}$ - T curve shown in Fig. 8(b), a local maximum in magnetization was observed around 25 K under an applied magnetic field of 1 T and the transition temperature where the local maximum occurred was lowered as the magnitude of the applied magnetic field increased. According to the understanding achieved in the present work this behavior is considered to be due to the asymmetric exchange interactions at the corner sites. Symmetry arguments show that the direction of the component of magnetic moment of the corner atom in the base plane should be along the direction of broken symmetry, which is indicated for the different corner atoms in Fig. 10. As a consequence, when the temperature decreases below a critical temperature (the spin reorientation temperature) the magnetic moments of the Pr atoms in the base plane reorient in such a way that they partially cancel each other out, thus reducing the component of resultant total magnetization in the plane.

IV. CONCLUSIONS

The variation of magnetization with temperature of $\text{Pr}_6\text{Ni}_2\text{Si}_3$ and $\text{Pr}_5\text{Ni}_2\text{Si}_3$ single crystal alloys has been calculated using a nearest neighbor exchange interaction approximation. In $\text{Pr}_6\text{Ni}_2\text{Si}_3$ two types of Pr atoms were classified, “corner” and “edge,” based on the number of nearest neighbors. In $\text{Pr}_5\text{Ni}_2\text{Si}_3$ three types of Pr atoms were classified, “corner,” “edge,” and “center,” based on the number of nearest neighbors.



(a)



(b)

FIG. 9. (Color online) (a) Calculated M vs T curves for the $\text{Pr}_5\text{Ni}_2\text{Si}_3$ compound. Red/blue/cyan/green symbols represent the magnetization due to the Pr atoms at the center/edge(A)/edge(B)/corner sites, respectively. The black symbols are the sum of these four contributions, which correspond to the total magnetization of this compound. (b) The expected variation with temperature of the angle θ relative to the c axis of magnetic moments for each of the different types of Pr atom.

Magnetization versus temperature (M vs T) curves for each type of atom were calculated as well as the average magnetization versus temperature (M vs T) curve for the whole trigonal array. The calculations predicted Curie temperatures of 40 K for $\text{Pr}_6\text{Ni}_2\text{Si}_3$ and 48 K for $\text{Pr}_5\text{Ni}_2\text{Si}_3$, which are in agreement with experimental results, but with different temperature dependences of magnetization for the

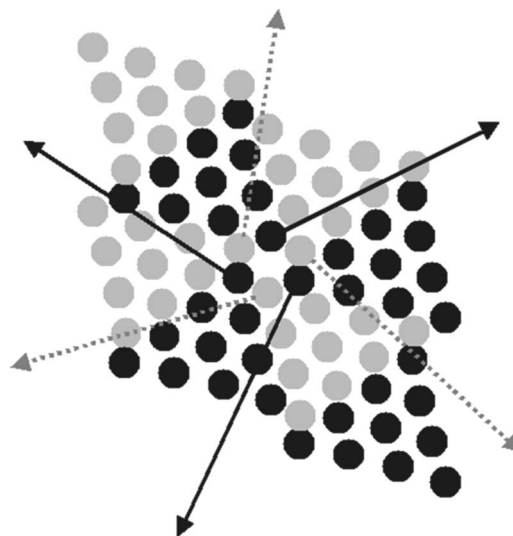


FIG. 10. Atomic arrangement of Pr atoms in the $\text{Pr}_5\text{Ni}_2\text{Si}_3$ compound. The arrows from the corner atoms indicate the direction in which the symmetry of the exchange interaction at the corner atom is broken.

different types of Pr atoms on corner, edge, and center sites. The results also showed that components of magnetic moments of Pr atoms at the corner sites have preferred orientation in the base plane with a sixfold symmetry. This sixfold preferred orientation in the base plane causes the component of magnetic moment in the base plane of each corner site to be partially canceled by the base plane components of magnetic moment of the other corner atoms, so that the resultant total magnetization was decreased. The critical temperature at which this occurs causes the second, or spin reorientation, transition to occur at about 25 K in $\text{Pr}_5\text{Ni}_2\text{Si}_3$, which has been observed experimentally.

ACKNOWLEDGMENTS

This research was supported by a Wolfson Research Fellowship from the Royal Society of the United Kingdom and by the U.S. Department of Energy, Office of Basic Energy Sciences, Materials Sciences Division. Ames Laboratory is operated for the U. S. Department of Energy by Iowa State University under Contract No. W-7405-ENG-82. The authors wish to thank Dr. R. W. McCallum for discussions concerning the results of this research.

¹P. Rogl, in *Handbook of the Physics and Chemistry of Rare Earths*, edited by K. A. Gschneidner, Jr. and L. R. Eyring (North-Holland, Amsterdam, 1987), Vol. 7, p. 1.

²A. O. Pecharsky, Y. Mozharivskyy, K. W. Dennis, K. A. Gschneidner, R. W. McCallum, G. J. Miller, and V. K. Pecharsky, *Phys. Rev. B* **68**, 134452 (2003).

³S. H. Song, D. C. Jiles, J. E. Snyder, A. O. Pecharsky, D. Wu, K. W. Dennis, T. A. Lograsso, and R. W. McCallum, *J. Appl. Phys.* **97**, 10M516 (2005).

⁴S. H. Song, J. E. Snyder, D. Wu, T. A. Lograsso, K. W. Dennis, R. W. McCallum, Y. Janssen, and D. C. Jiles, APS March Meeting, Los Angeles, 21–25 March 2005 (unpublished)

⁵S. H. Song, J. E. Snyder, D. Wu, T. A. Lograsso, K. W. Dennis, R. W. McCallum, Y. Janssen, and D. C. Jiles, *IEEE Trans. Magn.* **41**, 3499 (2005).

⁶D. C. Jiles *et al.*, *J. Magn. Magn. Mater.* **299**, 288 (2005).

⁷R. W. McCallum (private communication).

⁸A. Lobet Megias (private communication).